

TEM analysis of the TiC particles in aluminium containing AlTi3C0.15 grain refiner

I. Naglič^{1*}, A. Smolej², M. Doberšek¹

¹*Institute of Metals and Technology, Lepi pot 11, P.O. Box 431, SI-1000 Ljubljana, Slovenia*

²*University of Ljubljana, Faculty of Natural Sciences and Engineering, Aškerčeva cesta 12, 1000 Ljubljana, Slovenia*

Received 16 January 2007, received in revised form 25 May 2007, accepted 27 May 2007

Abstract

Determination of orientation relationships between TiC particles and the surrounding aluminium matrix using transmission electron microscopy is the main objective of this study. The melt of the commercial-purity aluminium and the commercial grain refiner AlTi3C0.15 were used to prepare experimental samples. Two orientation relationships between aluminium and TiC were found: $[111]_{\alpha\text{Al}} \parallel [111]_{\text{TiC}}$ and $(\bar{1}10)_{\alpha\text{Al}} \parallel (\bar{1}10)_{\text{TiC}}$, and $[114]_{\alpha\text{Al}} \parallel [110]_{\text{TiC}}$ and $(\bar{1}10)_{\alpha\text{Al}} \parallel (\bar{1}10)_{\text{TiC}}$. The $\{111\}$ planes of TiC and aluminium were found to be parallel what indicates the epitaxial nucleation of aluminium on $\{111\}$ planes of TiC.

Key words: solidification, aluminium, grain refining, orientation relationship

1. Introduction

It is well known that metals and alloys solidify usually with a coarse, columnar grain structure under normal casting conditions. In industry, grain refinement is a common way of achieving a proper, uniform, fine grain microstructure in aluminium alloys. The most widely used grain refiners are based on the Al-Ti-B system, notably Al-5wt.%Ti-1wt.%B. The AlTi5B1 grain refiners consist of the α_{Al} matrix, as well as Al_3Ti and TiB_2 particles [1]. Grain refiners based on the Al-Ti-B system are very effective, but they suffer from poisoning in the presence of Zr and some other elements [2]. An additional problem often mentioned is the agglomeration of particles. For the above reasons there is serious interest to use alternative grain refiners based on Al-Ti-C system, for example, the Al-3wt.%Ti-0.15wt.%C. The AlTi3C0.15 grain refiners are composed of the α_{Al} matrix, Al_3Ti and TiC particles [3]. It has been found that TiC is unstable phase at conditions typical for grain refinement at low temperatures and short holding times [4–6] but the rate of replacement of TiC by Al_4C_3 is rather slow and does not affect significantly the process of grain refinement. The TiC particles, introduced into the aluminium alloys via Al-Ti-C-based grain refiners, were

found in centres of the aluminium grain [7]. Mayes et al. [8] found out that the individual TiC particles in an AlTi6C0.02 grain refiner were single crystals with a characteristic octahedral morphology. Cisse et al. [9] studied that aluminium nucleates at TiC, and the orientation of the aluminium with respect to the TiC is completely epitaxial: $(001)_{\text{Al}} \parallel (001)_{\text{TiC}}$ and $[001]_{\text{Al}} \parallel [001]_{\text{TiC}}$. In their transmission electron microscopy (TEM) study, Mayes et al. [8] attempted to find TiC particles in the grain centres of the AlTi6C0.02 grain-refined aluminium. However, they did not find any TiC particles in centres of grains and concluded that a possibility to find a suitable particle in the thin foil is very low [8]. Tronche and Greer [10] studied commercial-purity aluminium treated with the commercial AlTi3C0.15 grain refiner using scanning electron microscopy (SEM) and electron backscatter diffraction (EBSD) techniques. They found out [10] that the grain centre of TiC particles, in terms of crystallographic orientation, matches the matrix fulfilling the orientation relationship proposed by Cisse et al. [9].

It can be assumed, based on the knowledge about orientation relationship between TiC and aluminium [9, 10], on the free growth criteria [11] and on the characteristic octahedral morphology of the TiC particles present in Al-Ti-C-based grain refiners [8] that the

*Corresponding author: tel.: +386 1 4701 922; fax: +386 1 4701 939; e-mail address: iztok.naglic@imt.si

Table 1. Chemical composition of the aluminium and the grain refiner in wt.%

Element	Si	Fe	V	B	Ti	C	Al
99.8 wt.% Al	0.031	0.081	0.001	< 0.0005	0.0015	–	bal.
Grain refiner	–	–	–	–	2.7	0.16	bal.

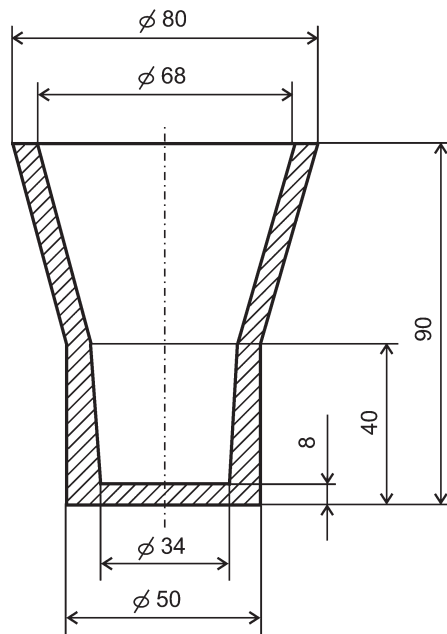


Fig. 1. The shape and dimensions of the bronze mould.

nucleation of aluminium takes place on the $\{111\}_{\text{TiC}}$ planes of the TiC in such a way that the $\{111\}$ planes in both the TiC and the aluminium are in parallel. The main aim of the present study was to give experimental (TEM) evidence about this assumption.

2. Experimental

Aluminium of commercial purity (99.8 wt.% Al) and the commercial grain refiner AlTi3C0.15 were used in this study. Chemical compositions of the aluminium and the grain refiner are presented in Table 1.

The aluminium (910 g) was melted in a corundum crucible in an electrical-resistance chamber furnace. A total of 33.3 g kg^{-1} of AlTi3C0.15 grain refiner was added at 705°C . After the addition of the grain refiner the melt was stirred, and three minutes after the addition of the grain refiner the melt was cast into a bronze mould, as shown in Fig. 1.

The casting was cut 13 mm above its base for the metallographic examination. Metallographic samples for light microscopy and SEM were ground and polished with diamond paste. The SEM examinations were performed with a JEOL-6500F equipped with EDS and WDS at 10 kV.

A thin plate was cut from the casting for preparation of TEM samples. The plate was mechanically thinned to approximately $10 \mu\text{m}$ by dimpling. The final thinning involved ion milling in a Bal-Tec RES010 with Ar. The TEM examinations were performed in a JEOL JEM 2010F transmission electron microscope equipped with an Oxford instruments ISIS 300 EDXS energy-dispersive X-ray spectrometer at 200 kV.

3. Results

3.1. SEM analysis

The results of SEM–WDS and SEM–EDS analyses presented in Fig. 2 show that the TiC particles are present in the central regions of the aluminium grains. It is well known that the equilibrium partitioning coefficient, k_{Ti} , of titanium in aluminium is 7.5 [1]. For this reason it is expected that the concentration of Ti in the solid solution of α_{Al} will decrease with increasing distance from the starting point of the solidification. This expectation was also confirmed experimentally as follows from Fig. 2 showing the decrease of titanium concentration in the solid solution of α_{Al} with increasing distance from the TiC agglomerate. It can be concluded, based on the titanium distribution in the solid solution of the α_{Al} grain, that the solidification started at the TiC agglomerate.

3.2. TEM analysis

In Fig. 3a a TEM image is shown of the TiC particle in the α_{Al} matrix. The diffraction patterns of the TiC particle and the α_{Al} matrix are presented in Fig. 3b. The indexed diffraction pattern in Fig. 3c shows that the zone axis in both the TiC particle and the α_{Al} matrix is $[111]$. In Fig. 3 the orientation relationship between the α_{Al} matrix and TiC particle is shown: $[111]_{\alpha_{\text{Al}}} \parallel [111]_{\text{TiC}}$ and $(\bar{1}10)_{\alpha_{\text{Al}}} \parallel (\bar{1}10)_{\text{TiC}}$.

In Fig. 4, another TiC particle is shown. It was confirmed that there is an increased concentration of titanium and carbon in the particle.

The TEM image of the TiC particle analysed in Fig. 4 is presented in Fig. 5. Diffraction patterns corresponding to both TiC and α_{Al} matrix are documented in Fig. 5b. The indexed diffraction patterns illustrated in Fig. 5c show zone axes: $[114]_{\alpha_{\text{Al}}} \equiv [110]_{\text{TiC}}$. The following orientation rela-

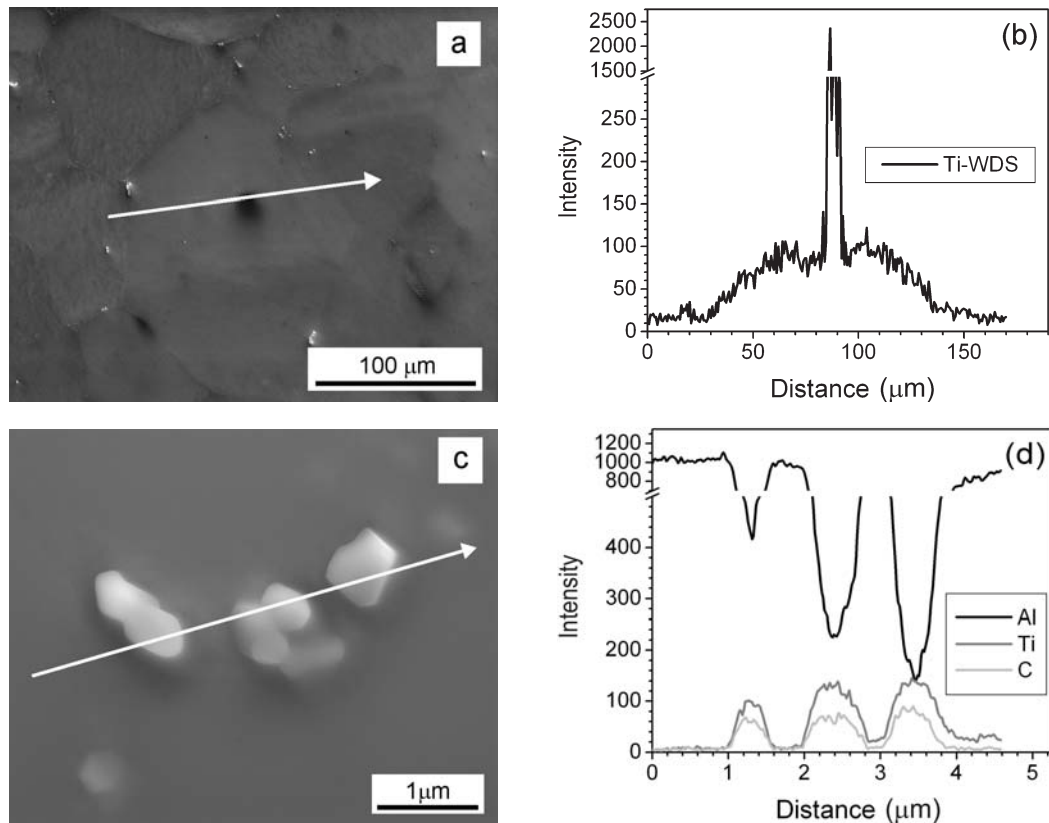


Fig. 2. SEM-WDS analysis of casting: a) SEM micrograph in secondary electrons; the arrow indicates the region of the WDS line-scan done for Ti; b) the intensity of the titanium $K\alpha$ X-ray radiation along the arrow; SEM-EDS analysis of the grain centre; c) SEM micrograph in secondary electrons with an arrow indicating the region of the EDS line-scan done for Al, Ti and C; d) intensities of Al, Ti and C $K\alpha$ X-ray radiations along the arrow.

tionship between α_{Al} matrix and TiC particle was found: $[114]_{\alpha_{\text{Al}}}\parallel[110]_{\text{TiC}}$ and $(\bar{1}10)_{\alpha_{\text{Al}}}\parallel(\bar{1}10)_{\text{TiC}}$.

4. Discussion

The orientation relationship $[111]_{\alpha_{\text{Al}}}\parallel[111]_{\text{TiC}}$ and $(\bar{1}10)_{\alpha_{\text{Al}}}\parallel(\bar{1}10)_{\text{TiC}}$ presented in Fig. 3 shows that the $[111]$ directions in both the TiC particle and the α_{Al} matrix are in parallel. This orientation relationship can be explained by epitaxial nucleation of aluminium on $\{111\}$ planes of TiC.

The $[110]$ directions in the TiC particle and the $[114]$ directions in the α_{Al} matrix are also parallel, Fig. 5. It can be shown that in cubic lattice the angle β_1 between directions $[110]$ and $[114]$ is equal to the angle β between (111) and $(1\bar{1}\bar{1})$ planes (Fig. 6): $\beta = \beta_1 = 70.53^\circ$ means, that identical $\{111\}$ planes in TiC and aluminium are in parallel.

As presented above, two different orientation relationships exist between α_{Al} and TiC. Both can be explained by nucleation of aluminium on $\{111\}$ planes of TiC in a way that the identical $\{111\}$ planes in the crystals are in parallel. Existence of orientation relationship $[114]_{\alpha_{\text{Al}}}\parallel[110]_{\text{TiC}}$ and $(\bar{1}10)_{\alpha_{\text{Al}}}\parallel(\bar{1}10)_{\text{TiC}}$

presented in Fig. 5 which is different than already known orientation relationship $(001)_{\text{Al}}\parallel(001)_{\text{TiC}}$ and $[001]_{\text{Al}}\parallel[001]_{\text{TiC}}$ (often called cube-cube) is a consequence of nucleation of aluminium on $\{111\}$ plane of TiC. Plane $\{111\}$ in TiC and aluminium shows 6-fold symmetry as can be also seen from diffraction pattern in Fig. 3b. Crystal structures themselves show only 3-fold symmetry about zone axes $\langle 111 \rangle$. Consequently there are two possible orientations of aluminium forming on octahedral TiC with atomic matching in the interface plane $\{111\}$. These two orientations are twin-related and can be presented by the rotation of one crystal about $\langle 111 \rangle$ direction for 60° (6-fold symmetry of $\{111\}$ planes and only 3-fold symmetry of crystal structure about zone axes $\langle 111 \rangle$). Existence of two twin-related orientations is consequence of nucleation of aluminium on $\{111\}$ faces of octahedral TiC particles. It is important to mention that in the case of cubic shape particles bounded by $\{100\}$ planes, for example nucleation of aluminium on $\{100\}$ planes, would not lead to twin-related orientations and only cube-cube orientation relationship between aluminium and TiC would exist.

It is also interesting to consider the disregistry, δ , between the TiC and the α_{Al} matrix. The disregistry

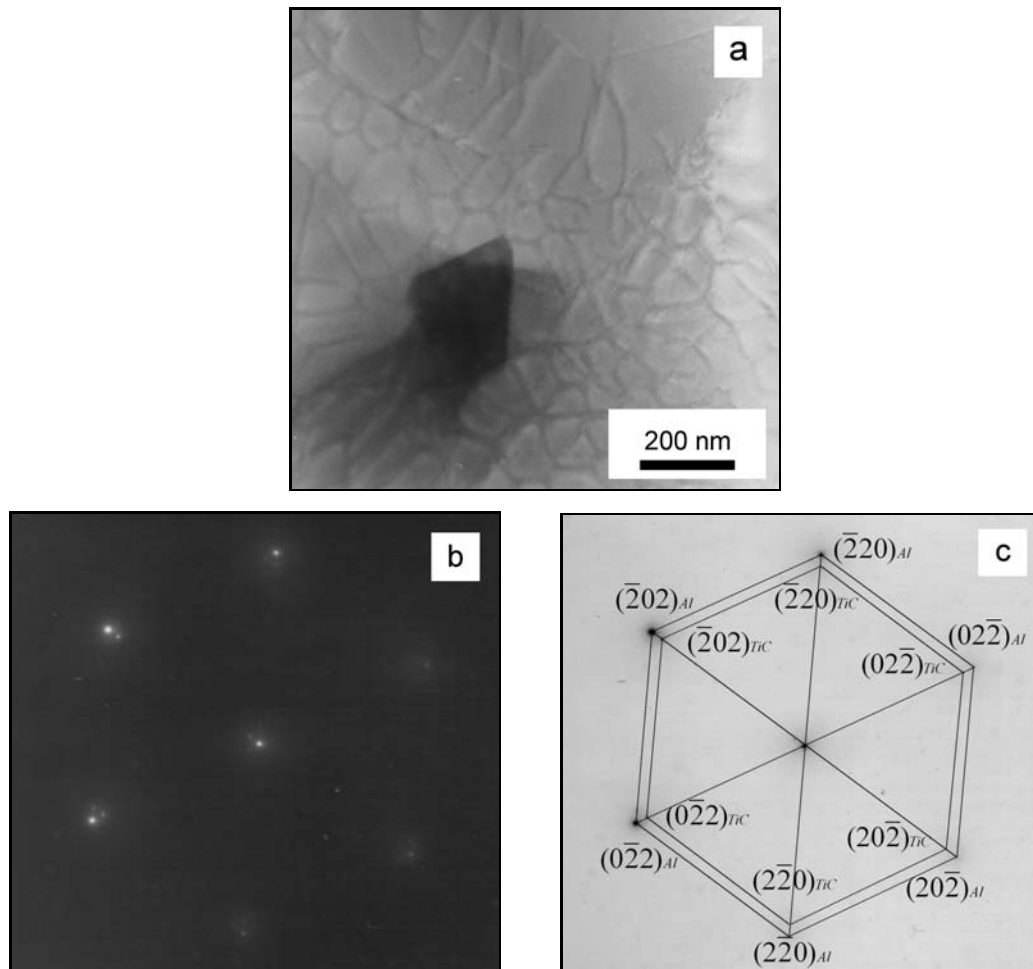


Fig. 3. a) TEM image of the TiC particle in the α_{Al} matrix; b) diffraction pattern corresponding to the TiC particle and the α_{Al} matrix; c) indexed diffraction patterns. Zone axes are: $[111]_{\alpha_{Al}} \equiv [111]_{TiC}$.

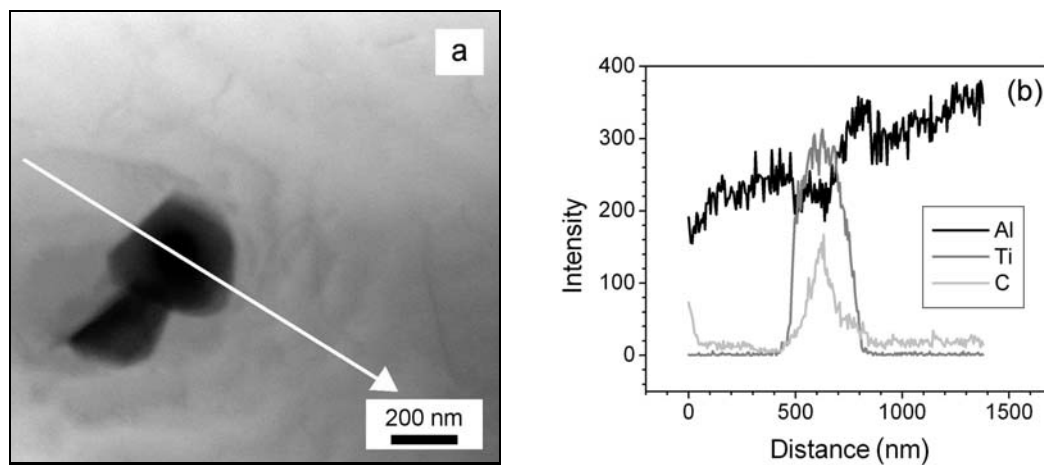


Fig. 4. a) TEM image of TiC particle with marked region of the EDS line-scan; b) the distribution of Al, Ti and C along the scanned region.

calculated based on the known lattice parameters of the aluminium $a_{Al} = 0.405$ nm and the TiC $a_{TiC} = 0.433$ nm is $\delta = 0.065$. The discrepancy calculated from the measured distances between the $\{220\}$ diffraction

spots on the negatives of the diffraction patterns is $\delta = 0.070$. The difference between the theoretical and the experimental values of the lattice discrepancy is negligible.

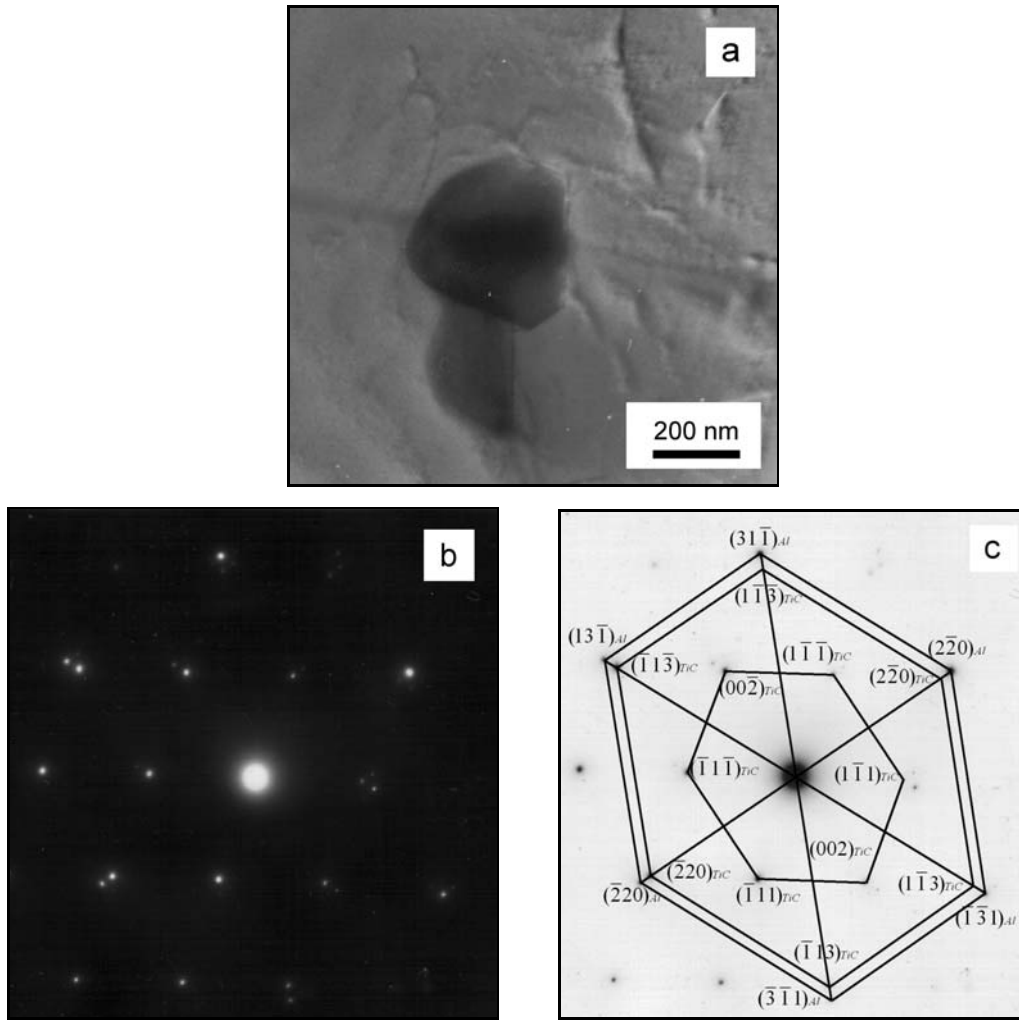


Fig. 5. a) TEM image of the TiC particle present in the α_{Al} matrix; b) diffraction pattern corresponding to the TiC particle and the α_{Al} matrix; c) indexed diffraction patterns. Zone axes are: $[114]_{\alpha_{Al}} \equiv [110]_{TiC}$.

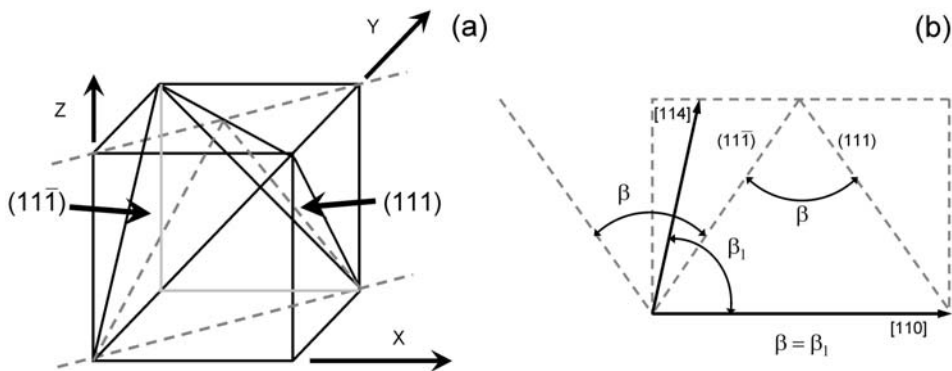


Fig. 6. a) Elementary cell of a cubic crystal illustrating intersection of the $(\bar{1}10)$ plane with planes (111) and $(11\bar{1})$; b) the angles between $[114]$ and $[110]$ directions and (111) and $(11\bar{1})$ planes are shown in projection plane $(\bar{1}10)$.

The EDS line-scan in Fig. 4 shows the distribution of Al, Ti and C in the TiC particle and gives evidence about presence of Ti and C in the particle. It can be seen that the C peak at the centre of the TiC particle is sharper than the Ti peak. This might

mean that the C/Ti ratio is not constant across the TiC particle, but increases from the α_{Al}/TiC interface to the centre of the particle. It has been shown [12] that TiC particles in Al-Ti-C composites can be non-stoichiometric $TiC_{0.8}$ compounds. Cisse et al. [9]

mentioned that carbon depletion in outer parts of the TiC would lower the misfit between the TiC and the aluminium.

5. Conclusions

On the basis of the titanium distribution in the solid solution of the α_{Al} we found that in aluminium with the addition of AlTi3C0.15 grain refiner the solidification starts on agglomerates of TiC particles.

The TiC particles in aluminium with the addition of the AlTi3C0.15 grain refiner are in an orientation relationship with the surrounding α_{Al} . Two orientation relationships were found: $[111]_{\alpha_{\text{Al}}}\parallel[111]_{\text{TiC}}$ and $(\bar{1}10)_{\alpha_{\text{Al}}}\parallel(\bar{1}10)_{\text{TiC}}$, and $[114]_{\alpha_{\text{Al}}}\parallel[110]_{\text{TiC}}$ and $(\bar{1}10)_{\alpha_{\text{Al}}}\parallel(\bar{1}10)_{\text{TiC}}$. Both crystallographic relationships can be explained assuming that the nucleation of aluminium takes place on the $\{111\}$ planes of the TiC in such a way that the identical $\{111\}$ planes in both crystals are in parallel.

References

- [1] McCARTNEY, D. G.: International Materials Reviews, *34*, 1989, p. 247.
- [2] MURTY, B. S.—KORI, S. A.—CHAKRABORTY, M.: International Materials Reviews, *47*, 2002, p. 3.
- [3] GREER, L. A.—COOPER, P. S.—MEREDITH, M. W.—SCHNEIDER, W.—SCHUMACHER, P.—SPITTLER, J. A.—TRONCHE, A.: Advanced Engineering Materials, *5*, 2003, p. 81.
- [4] SATO, K.—FLEMINGS, M. C.: Metallurgical and Materials Transactions A, *29A*, 1998, p. 1707.
- [5] VANDYOUSSEFI, M.—WORTH, J.—GREER, A. L.: Materials Science and Technology, *16*, 2000, p. 1121.
- [6] TRONCHE, A.—VANDYOUSSEFI, M.—GREER, A. L.: Materials Science and Technology, *18*, 2002, p. 1072.
- [7] BANERJI, A.—REIF, W.: Metallurgical Transactions A, *17A*, 1986, p. 2127.
- [8] MAYES, C. D.—McCARTNEY, D. G.—TATLOCK, G. J.: Materials Science and Engineering A, *A188*, 1994, p. 283.
- [9] CISSE, J.—BOLLING, G. F.—KERR, H. W.: Journal of Crystal Growth, *13/14*, 1972, p. 777.
- [10] TRONCHE, A.—GREER, A. L.: Philosophical Magazine Letters, *81*, 2001, p. 321.
- [11] GREER, A. L.—BUNN, A. M.—TRONCHE, A.—VANS, P. V.—BRISTOW, D. J.: Acta Materialia, *48*, 2000, p. 2823.
- [12] TONG, X. C.—FANG, H. S.: Metallurgical and Materials Transaction A, *29A*, 1998, p. 875.